



6 Şubat 2023 Türkiye Depremleri Sonrası Hasar Görmüş Yollardan Elde Edilen Asfalt Bağlayıcılarının Fiziksel ve Reolojik Özelliklerindeki Bölgesel Farklılıklar

Beyza FURTANA YALCIN^{1*}  

¹Inşaat Mühendisliği Bölümü, Mühendislik Fakülte, Munzur Üniversite, Tunceli, Türkiye.
¹beyzafurtana@munzur.edu.tr

Geliş Tarihi: 15.08.2025
Kabul Tarihi: 18.09.2025

Düzeltilme Tarihi: 14.09.2025

doi: <https://doi.org/10.62520/fujece.1766725>
Araştırma Makalesi

Alıntı: A. M. Özdemir, "6 Şubat 2023 türkiye depremleri sonrası hasar görmüş yollardan elde edilen asfalt bağlayıcılarının fiziksel ve reolojik özelliklerindeki bölgesel farklılıklar", Fırat Üni. Deny. ve Hes. Müh. Derg., vol. 4, no 3, pp. 657-669, Ekim 2025.

Öz

Bu çalışma, 6 Şubat 2023'te Güneydoğu Türkiye'de meydana gelen ($M_w = 7.8$ ve $M_w = 7.5$) depremler sonrasında Hatay, Kahramanmaraş, Gaziantep ve Malatya'daki hasar görmüş yol kesimlerinden alınan asfalt karışım numunelerinden elde edilen bağlayıcıların fiziksel ve reolojik özelliklerini incelemektedir. Şiddetli bozulmaların gözlemlendiği kaplamalardan alınan numunelerden, çözücü ekstraksiyonu ve rotary evaporasyon yöntemleri ile bitüm geri kazanılmıştır. Geri kazanılan bağlayıcılar; yaşlanma, sertlik, yüksek sıcaklık performansı ve viskoelastik davranışlarını değerlendirmek amacıyla penetrasyon, yumuşama noktası, dönel viskozite ve Dinamik Kesme Reometresi (DSR) deneylerine tabi tutulmuştur. Sonuçlar, bölgeler arasında belirgin farklılıklar olduğunu göstermiştir: Hatay bağlayıcıları en düşük penetrasyon, en yüksek yumuşama noktası, en yüksek viskozite ve en yüksek tekerlek izi direncine (yüksek $G^*/\sin\delta$ değerleri) sahip olup, daha düşük faz açıları ile yüksek sıcaklıklarda dahi elastikiyetini korumuştur. Buna karşılık Kahramanmaraş bağlayıcıları en yüksek penetrasyon, en düşük yumuşama noktası, düşük viskozite ve yüksek faz açıları ile daha yumuşak, daha viskoz bir yapı sergilemiş ve yüksek sıcaklıklarda kalıcı deformasyona karşı daha düşük direnç göstermiştir. Malatya ve Gaziantep bağlayıcıları ise ara özellikler sunmuş; Malatya bağlayıcıları orta sertlikte, Gaziantep bağlayıcıları ise daha yüksek esnekliğini koruyan yapıda bulunmuştur. Tüm numunelerde sıcaklık arttıkça viskozite değerleri önemli ölçüde azalmış, DSR sonuçları ise yüksek sıcaklıklarda tekerlek izi direncinin düştüğünü, ancak başlangıçta yüksek $G^*/\sin\delta$ değerine sahip bağlayıcıların performansını daha iyi koruduğunu ortaya koymuştur. Bulgular, yerel deprem şiddeti, iklim koşulları ve kaplama kullanım geçmişinin deprem sonrası bağlayıcı davranışı üzerinde doğrudan etkili olduğunu ve afet sonrası bakım-onarım stratejilerinin her bölgenin özgün malzeme özelliklerine göre uyarlanması gerektiğini vurgulamaktadır.

Anahtar kelimeler: Asfalt bağlayıcı, Deprem sonrası yol hasarı, Reolojik özellikler, Yüksek sıcaklık performansı

*Yazışılan yazar



Regional Variations in the Physical and Rheological Properties of Asphalt Binders Recovered from Earthquake-Damaged Roads Following the February 6, 2023 Türkiye Earthquakes

Beyza FURTANA YALCIN^{1*}  

¹Department of Civil Engineering, Faculty of Engineering, Munzur University, Tunceli, Türkiye.
beyzafurtana@munzur.edu.tr

Received: 15.08.2025
Accepted: 18.09.2025

Revision: 14.09.2025

doi: <https://doi.org/10.62520/fujece.1766725>
Research Article

Citation: B. Furtana Yalçın, "Regional variations in the physical and rheological properties of asphalt binders recovered from earthquake-damaged roads following the february 6, 2023 türkiye earthquakes", *Firat Univ. Jour. of Exper. and Comp. Eng.*, vol. 4, no 3, pp. 657-669, October 2025.

Abstract

This study investigates the physical and rheological properties of asphalt binders recovered from earthquake-damaged road sections in Hatay, Kahramanmaraş, Gaziantep, and Malatya following the February 6, 2023, earthquakes in southern Türkiye ($M_w = 7.8$ and $M_w = 7.5$). Asphalt mixture samples were collected from severely deteriorated pavements, and bitumen was extracted through solvent extraction and rotary evaporation. The recovered binders were subjected to penetration, softening point, rotational viscosity, and Dynamic Shear Rheometer (DSR) tests to evaluate aging, stiffness, high-temperature performance, and viscoelastic behavior. Results revealed significant regional differences: Hatay binders exhibited the lowest penetration, highest softening point, highest viscosity, and the greatest rutting resistance (high $G^*/\sin\delta$ values) while maintaining lower phase angles, indicating enhanced stiffness and elasticity. In contrast, Kahramanmaraş binders showed the highest penetration, lowest softening point, and lower viscosity, combined with high phase angles, reflecting a softer, more viscous character with reduced deformation resistance. Malatya and Gaziantep binders displayed intermediate characteristics, with Malatya showing moderate stiffness and Gaziantep retaining greater flexibility. Across all samples, viscosity decreased markedly with increasing temperature, and rutting resistance diminished at higher service temperatures; however, binders with higher initial $G^*/\sin\delta$ values retained better performance. The findings highlight the influence of regional seismic intensity, climatic conditions, and pavement history on binder behavior and emphasize the need for region-specific maintenance and rehabilitation strategies in post-disaster pavement management.

Keywords: Asphalt binder, Post-earthquake road damage, Rheological properties, High-temperature performance

*Corresponding author

1. Introduction

On February 6, 2023, two devastating earthquakes with magnitudes of 7.8 and 7.5 struck southern Türkiye, causing catastrophic damage to infrastructure, including residential buildings, bridges, transportation systems, and other critical lifelines. Severe ground deformations such as landslides, fault ruptures, and subsidence further amplified the destruction [1-2]. Major cities, including Kahramanmaraş, Hatay, and Gaziantep, with a combined population of approximately 15 million, were heavily impacted, resulting in nearly 50.000 fatalities and the collapse of more than 19.000 buildings [3-4].

While numerous studies have addressed the seismic performance of buildings and historical structures in the affected region [5-7], limited attention has been paid to the post-earthquake condition of highway pavements. This is a critical gap, as highways are essential for emergency response and the delivery of humanitarian aid in disaster zones. Earthquake-induced damage to asphalt pavements often manifests as cracking, which can be active or inactive, and includes transverse, longitudinal, and alligator cracks [8-11]. Such cracks, if not promptly repaired, can accelerate deterioration by allowing moisture infiltration, ultimately reducing pavement service life.

Recent advancements in computer vision and deep learning have opened new possibilities for rapid, reliable, and automated crack detection, offering clear advantages over manual inspections, which are time-consuming and error-prone [12-16]. Several studies have explored automated crack detection specifically in the context of the 2023 Kahramanmaraş earthquakes. Demir et al. introduced a deep learning-based classification framework employing a customized multi-scale, multi-input ConvMixer architecture with gradient-based preprocessing, achieving a classification accuracy of 94.2% for post-earthquake asphalt cracks categorized as major or minor [17]. Yılmaz et al. developed a unique crack image dataset from heavily affected provinces, classifying cracks into urgent and non-urgent maintenance categories. They evaluated several pre-trained CNN models and improved classification accuracy to 80.32% using a Combined Metaheuristic Optimization-ReliefF (CMO-R) approach. In addition to classification, semantic segmentation methods have been applied for pixel-level crack detection [18]. Yılmaz et al. created a high-accuracy, pixel-labeled dataset from highways affected by the February 6 earthquakes and evaluated multiple deep learning-based segmentation models. SegNet achieved the highest performance, with an accuracy of 86.72%, precision of 92.99%, and sensitivity of 78.45%, outperforming conventional methods and demonstrating the potential for real-time infrastructure monitoring in disaster-prone regions [19].

These recent contributions emphasize the increasing significance of automated crack detection and classification in post-disaster infrastructure management, where rapid and reliable assessments are critical for ensuring mobility, safety, and the timely delivery of emergency aid. Nevertheless, despite notable progress, current approaches still face limitations, particularly in terms of segmentation precision, robustness under diverse field conditions, and the integration of laboratory-based rheological data with image-based distress evaluation. Addressing these gaps requires the development of more comprehensive frameworks that combine field investigations, advanced computational methods, and engineering judgment to improve decision-making in prioritizing maintenance and rehabilitation. Building upon the existing literature, the present study extends the scope of research by performing detailed on-site investigations of earthquake-induced pavement distress in Kahramanmaraş, systematically extracting and analyzing asphalt binder properties, and applying advanced segmentation techniques to classify and spatially map crack types. By linking material-level characterization with image-based crack detection, the study offers a more holistic understanding of seismic impacts on pavement systems and provides actionable insights to support post-earthquake highway maintenance strategies, resilience planning, and the design of more durable infrastructure in seismically active regions.

While recent studies have predominantly concentrated on the automated detection and classification of post-earthquake pavement cracks using image-based approaches, they have not provided a direct evaluation of the underlying material properties of the affected asphalt layers. In contrast, the present study introduces a distinctive experimental methodology by directly collecting asphalt mixture samples from severely damaged road sections in Hatay, Kahramanmaraş, Gaziantep, and Malatya following the devastating February 6, 2023, earthquakes. The extracted bitumen, recovered through standardized solvent extraction and rotary

evaporation procedures, was subjected to a comprehensive set of laboratory analyses, including penetration, softening point, and viscosity tests, alongside rheological characterization through DSR measurements. This dual approach, combining material-level binder evaluation with the broader context of seismic pavement distress, offers an unprecedented link between field-scale damage manifestations and intrinsic binder performance.

Such an integrated perspective enables not only the quantitative assessment of earthquake-induced aging and degradation mechanisms but also a deeper understanding of how seismic forces accelerate binder hardening, reduce elasticity, and compromise high-temperature rutting resistance. By systematically comparing samples from multiple regions, the study highlights the influence of local seismic intensity, traffic loading, and climatic variations on binder performance, thereby revealing regional disparities that have not been addressed in earlier research. Ultimately, this novel framework bridges the gap between surface-level crack identification and the intrinsic durability of asphalt materials, providing both the scientific community and infrastructure agencies with actionable insights to design more resilient pavements and to establish tailored post-disaster maintenance strategies.

2. Materials and Methods

2.1. Pure binder

In this study, B 70/100-grade bitumen, one of the most commonly used virgin binder types in Turkey, was selected as the reference binder and was supplied by the TUPRAS Batman Refinery. The general properties of the bitumen used in the study are provided in Table 1.

Table 1. General properties of 70/100 bitumen

Properties	Unit	Standard	Results
Penetration	mm ⁻¹	EN 1426	87.4
Softening Point	°C	EN 1427	52.6
Flash Point	°C	EN ISO 2719	230
Viscosity 135°C /165°C	cP	ASTM D4402	562.5/162.5

2.2. Properties of the reclaimed asphalt pavement (RAP) material

Reclaimed asphalt pavement (RAP) materials were sampled in accordance with the EN 932-1 standard (TS EN 932-1, 1997). To assess the aggregate gradation of the RAP, an extraction procedure was conducted (Figure 1a). The aged binder obtained from the RAP through this extraction process was recovered using a rotary evaporator, following the TS EN 12697-3+A1 standard (2019) (Figure 1b). The bitumen content was quantified by conducting a total of 50 extraction tests. Throughout the experimental program, the recovered aged binder served as the primary binder material [20-22].

Samples were taken from the provinces of Hatay, Kahramanmaras, Gaziantep, and Malatya. The samples from Hatay, Kahramanmaras, Gaziantep, and Malatya were labeled with the letters H, K, G, and M, respectively. The numbers next to these names in the article indicate that they were taken from different regions. Examples of asphalt deformations by province are given in Figure 2.

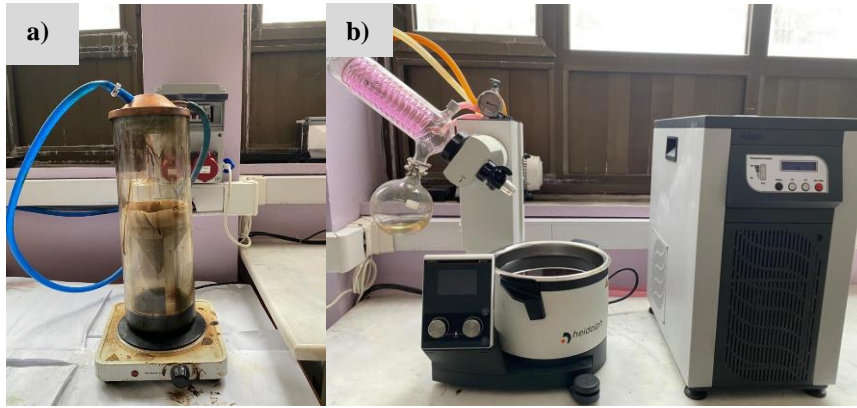


Figure 1. a) Extraction device b) rotary evaporator

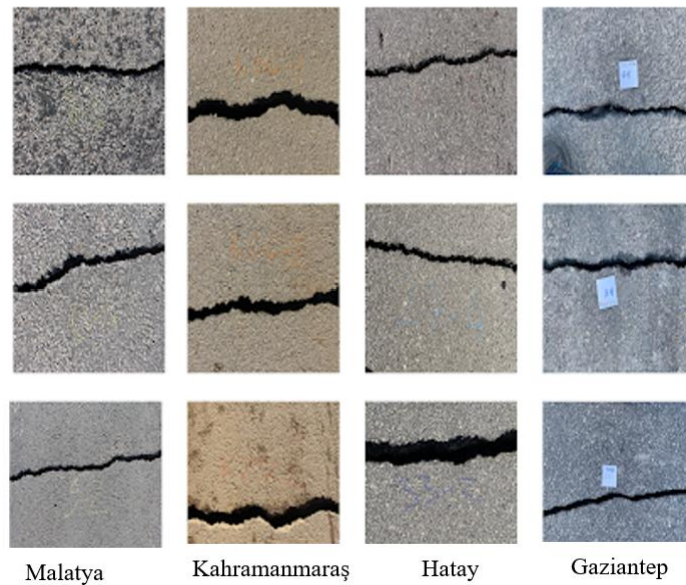


Figure 2. Sample images of asphalt deformations by province

2.3. Penetration test

It is a test method used to determine the hardness, i.e., the consistency, of a bituminous binder. It is expressed as the depth (in tenths of a millimeter) to which a standard needle penetrates a bitumen sample under a 100 g load at 25 °C for 5 seconds. The unit of the penetration value is 10^{-1} mm. There is an inverse relationship between the penetration values and the consistency of bituminous binders. An increase in the penetration value of a bitumen sample indicates a decrease in its consistency, meaning it has begun to soften. Conversely, a decrease in the penetration value indicates an increase in consistency, meaning the bitumen has hardened. A penetration test was carried out according to the TS EN 1426 standard.

The sample to be subjected to the penetration test is first placed in an oven until it becomes fluid and, after being mixed to achieve homogeneity, is poured into the penetration container. The material in the container is then left to cool at 25 °C for 60–90 minutes. Subsequently, the sample is kept in a water bath at 25 °C (Figure 3) for another 60–90 minutes before being placed on the table of the penetration apparatus (Figure 4). A 100 g weighted needle is positioned so that it just touches the surface of the sample and is then released to penetrate for 5 seconds. The procedure is repeated three times, and the average of these values is recorded as the penetration value.



Figure 3. Water bath



Figure 4. Penetration testing device

2.4. Softening point test

This test is conducted to determine the softening temperature of bitumen. In the procedure, a standard ring apparatus is filled with bitumen, and a ball is placed on top from a height of 2.5 cm. The test begins at 5 °C, and the temperature is increased at a rate of 5 °C per minute. The softening point is defined as the temperature indicated on the thermometer at the moment the bitumen sample makes contact with the base. The softening point test was performed according to the TS EN 1427 standard.

If the measured softening temperature exceeds 80 °C, glycerin should be used instead of water as the test medium, and the initial temperature should be set to 32 °C. The softening point is particularly important for limiting rutting in asphalt mixtures with high binder content. There is a strong correlation between this parameter and deformation susceptibility; a decrease of 5–6 °C in the softening temperature has been reported to result in approximately 20% more rutting. The automatic softening point apparatus used in the test is shown in Figure 5.

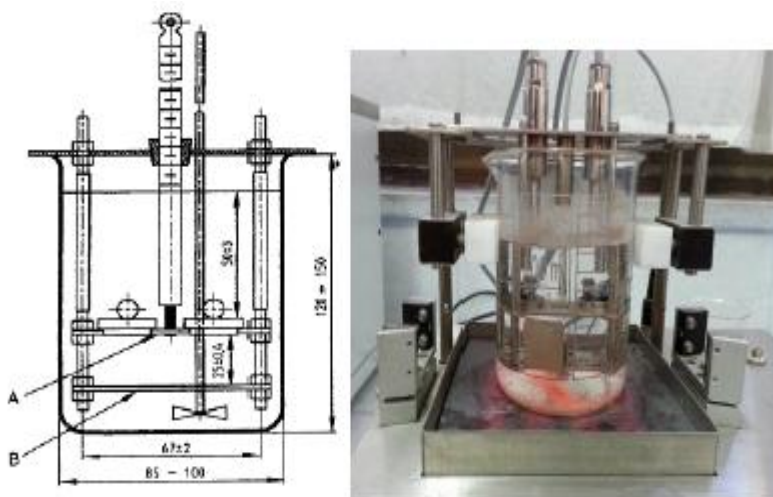


Figure 5. Softening point test setup

2.5. Rotational viscometer (RV) test

The Rotational Viscometer (RV) test is performed to evaluate the flow behavior of bituminous binders at high temperatures. In this test, a Brookfield-type viscometer, in compliance with the AASHTO T316 standard, is used (Figure 6). The viscosity values obtained are analyzed to determine whether the binder

provides sufficient fluidity during mixing and pumping processes. In the procedure, the spindle is rotated at a constant speed of 20 revolutions per minute by a motor, and the viscosity readings are recorded. The RV test, typically conducted on unaged binders, generally assumes that the viscosity at 135 °C should not exceed 3 Pa·s.



Figure 6. Viscometer test device

2.6. Dynamic shear rheometer test

The dynamic shear rheometer (DSR) test is employed to evaluate the viscous and elastic characteristics of bituminous binders at intermediate and high service temperatures. In this method, the complex shear modulus (G^*) and phase angle (δ) of the binder are measured. The complex shear modulus reflects the overall resistance of the binder to deformation under torsional loading within a specific time period, whereas the phase angle indicates the time lag between the application of shear stress and the resulting shear strain. A higher phase angle denotes a binder with a more viscous nature. According to performance criteria, the permanent deformation potential of unaged binders is controlled by ensuring that the $G^*/\sin\delta$ value does not exceed 1.0 kPa [23-24]. The tests were conducted using a Bohlin DSR-II rheometer on pure and modified bitumen according to ASTM D7175 standards. The tests were also conducted with a plate with a 25 mm diameter and 1 mm plate clearance at 1.59 Hz frequency value, and at 52°C, 58°C, 64°C, 70°C, 76°C, 82°C, and 88°C. In the test, rutting parameters and phase angles were determined to evaluate the high-temperature performances and elastic behaviors of the binders.

3. Results and Discussion

3.1. Penetration test results

Penetration test results are given in Figure 7. The penetration test results indicate clear regional variations in binder hardness among the asphalt samples collected from earthquake-affected areas. The lowest penetration values were observed in H1 and H2 (Hatay), reflecting significant binder hardening and aging, likely caused by severe mechanical stresses, substantial temperature fluctuations, and intense ground movements following the earthquake. M2 and M1 (Malatya) exhibited moderate penetration values, suggesting less hardening compared to Hatay. G1 and G2 (Gaziantep) showed higher penetration values, indicating softer binders with lower levels of aging. The highest values were recorded for K1 and K2 (Kahramanmaras), suggesting that the binder retained much of its flexibility with minimal hardening. These differences can be attributed to variations in local ground motion intensity, traffic loading conditions, climatic influences, and the pre-existing structural state of the pavement layers. Overall, the findings highlight the necessity for post-earthquake maintenance and rehabilitation strategies to be tailored to the specific material performance characteristics of each region, rather than relying on a uniform repair approach.

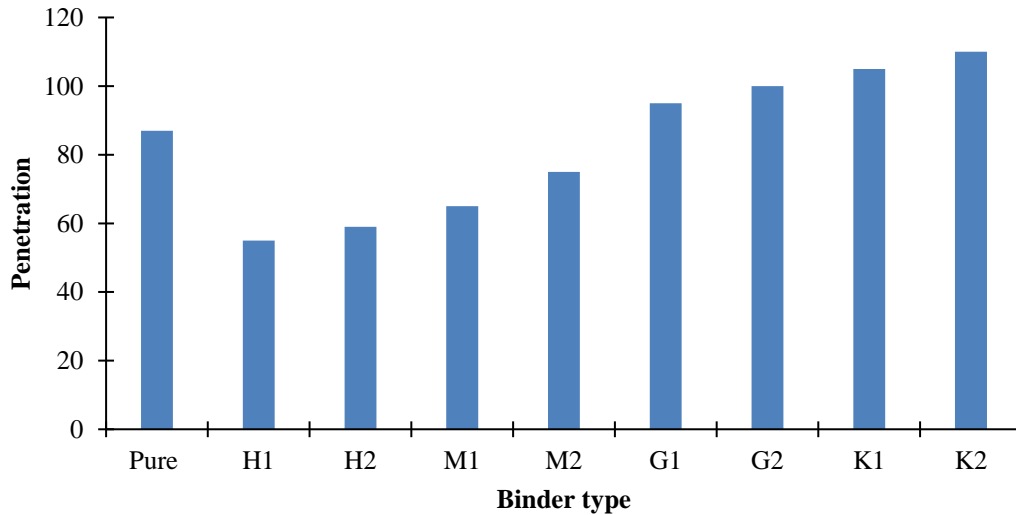


Figure 7. Penetration test results

3.2. Softening point test results

The softening point test results are given in Figure 8. The softening point test results reveal notable variations in high-temperature performance among asphalt binders collected from different earthquake-affected regions. The highest softening point was observed in H1 (Hatay), indicating significant hardening of the binder and enhanced resistance to deformation at elevated temperatures. H2, M2, and M1 samples exhibited moderate softening points, reflecting partial hardening effects. In contrast, G1 and G2 (Gaziantep) and K1 and K2 (Kahramanmaras) showed lower softening point values, suggesting that these binders tend to flow more easily at high temperatures and have retained a degree of elasticity. These differences can be attributed to regional variations in temperature fluctuations, traffic loading conditions, and the intensity of mechanical stresses induced by the earthquake. Overall, the findings highlight that high-temperature performance varies by region, and such differences should be taken into account when planning maintenance and rehabilitation strategies.

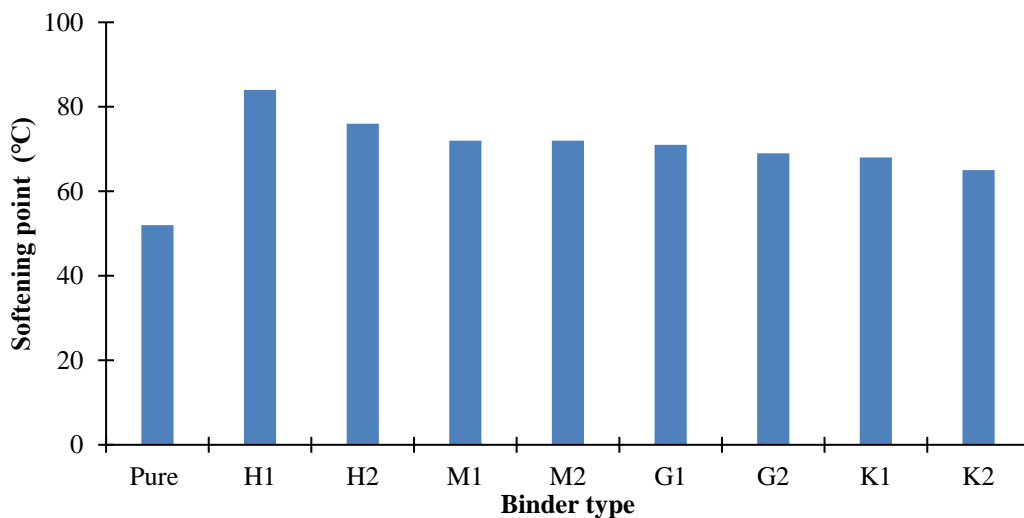


Figure 8. Softening point test results

3.3. Viscosity test results

Viscosity test results are given in Figure 9. The viscosity test results reveal significant regional variations in the high-temperature performance of asphalt binders collected from earthquake-affected areas. At 135

°C, the highest viscosity values were recorded for H1 (4800 cP) and H2 (4675 cP), indicating substantial hardening of the binder and markedly low fluidity even at elevated mixing temperatures. Such high-viscosity binders can lead to increased energy consumption during production, workability challenges during mixing and paving, and potential compaction issues if not adequately heated. M2 (2850 cP), G1 (3125 cP), K1 (3250 cP), and K2 (3350 cP) exhibited moderate viscosity values, while M1 (1538 cP) and G2 (1475 cP) showed the lowest readings, suggesting that these binders have undergone less aging and retain greater flowability.

At 165 °C, viscosity values decreased significantly for all samples. H1 and H2 dropped to 875 cP and 825 cP, respectively; M2 to 662.5 cP, M1 to 575 cP, G1 to 550 cP, G2 to 525 cP, K1 to 375 cP, and K2 to 350 cP. This reduction highlights the pronounced influence of temperature on binder workability. While higher temperatures improve flow and facilitate mixing and compaction, binders with high viscosity at lower temperatures may raise production costs and pose application challenges, particularly in colder climates where adequate spreading and compaction may be hindered.

These findings demonstrate that the rheological properties of asphalt binders vary considerably across regions following the earthquake, likely due to differences in local seismic intensity, traffic loads, climatic conditions, and pre-existing pavement characteristics. Consequently, post-earthquake maintenance and rehabilitation strategies should account for the temperature-dependent viscosity behavior of binders, with mixing and paving temperatures optimized to match regional conditions for improved performance and cost efficiency.

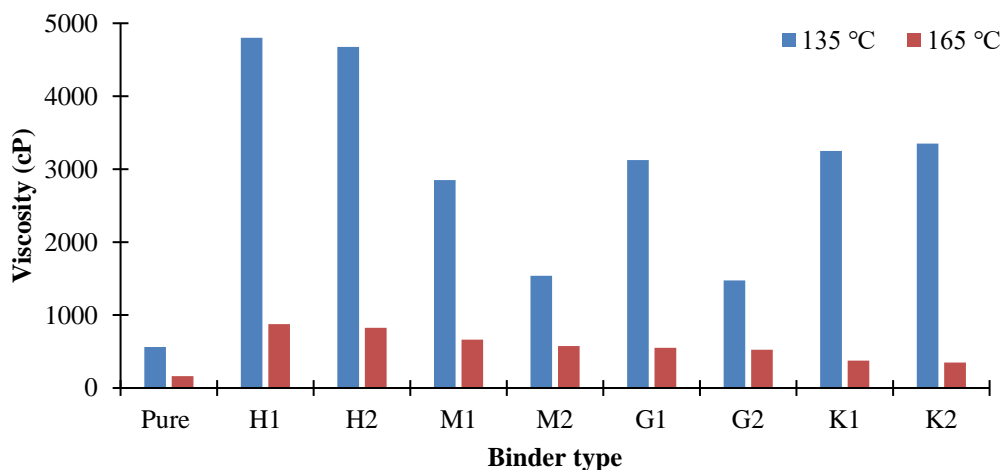


Figure 9. Viscosity test results

3.4. DSR test results

Figure 10 illustrates how the rutting parameter values of the binders vary with increasing temperature. The $G^*/\sin\delta$ results obtained from the DSR test provide a measure of the binders' resistance to permanent deformation at high service temperatures. In general, all samples exhibited a clear decrease in $G^*/\sin\delta$ values as the temperature increased, reflecting reduced stiffness and rutting resistance at higher service temperatures. At 52 °C, the highest value was recorded for H1 (1.90×10^5 Pa), followed by H2 (1.76×10^5 Pa) and M1 (1.61×10^5 Pa). These results suggest that certain binders from Hatay and Malatya maintained high rigidity even at relatively high temperatures, indicating strong rutting resistance. Conversely, the lowest initial value was observed for K2 (8.85×10^4 Pa), indicating a softer binder more prone to deformation at elevated temperatures. As the temperature increased to 58 °C, 64 °C, and 70 °C, all binders showed declining values, though H1 and H2 consistently remained higher than the others. At 76 °C, H1 and H2 still led with 1.08×10^4 Pa, while M2 (4669 Pa) and K2 (2735 Pa) dropped considerably. At 88 °C, all samples fell below 3000 Pa, with the lowest value again in K2 (638 Pa). This trend highlights that while stiffness decreases significantly at high temperatures for all binders, those with higher initial values maintain relatively better performance.

Overall, there are pronounced differences in high-temperature rutting resistance among the asphalt binders collected from different regions after the earthquake. Hatay samples (H1, H2) exhibit the highest stiffness and rutting resistance potential, while the K2 binder from Kahramanmaras has the lowest values. This underscores the influence of regional conditions, seismic severity, traffic loads, and aging levels on binder performance.

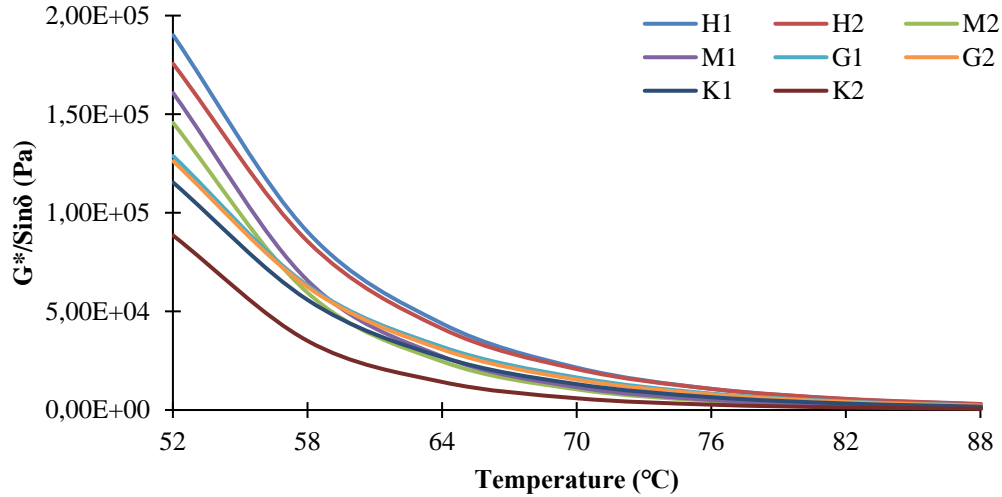


Figure 10. Variation of $G^*/\sin\delta$ values with temperature

Figure 11 shows the change in the phase angles of the binders with temperature. The phase angle (δ) values reflect the viscoelastic behavior of binders, indicating the balance between their elastic and viscous components. Overall, phase angle increased with temperature for all samples, suggesting a shift from predominantly elastic to more viscous behavior at higher service temperatures. At 52 °C, the lowest phase angles were observed for H1 (53.7°) and H2 (55.23°), indicating a higher elastic component and potentially greater resistance to deformation. The highest initial values were found for K1 (74.18°) and K2 (72.83°), showing that these binders displayed a more viscous character even at lower temperatures. At 64 °C and 70 °C, all samples continued to show increasing phase angles, with K1, K2, and G2 reaching the highest values, confirming their viscous-dominated behavior. In contrast, H1, H2, and M1 retained relatively lower phase angles, maintaining a greater degree of elasticity. At 88 °C, K1 (91.91°) and K2 (88.06°) recorded the highest phase angles, while H1 (75.94°) and H2 (76.09°) had the lowest, suggesting that Hatay binders preserved more elasticity under high temperatures, whereas Kahramanmaras binders became highly viscous. These results highlight clear regional differences in the elastic–viscous balance of asphalt binders collected after the earthquake, which are directly influenced by both temperature and the degree of material aging.

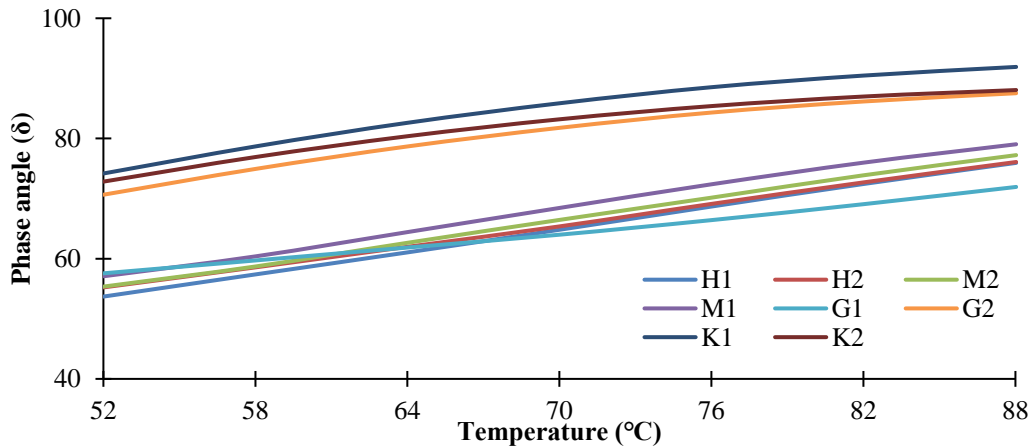


Figure 11. Variation of the phase angles of the binders with temperature

4. Conclusions

The results of penetration, softening point, viscosity, and DSR tests clearly demonstrate significant regional differences in the physical and rheological properties of asphalt binders collected from earthquake-affected areas, reflecting variations in aging, stiffness, and viscoelastic balance.

- Penetration, softening point, viscosity, and DSR tests demonstrated significant regional differences in the physical and rheological properties of asphalt binders collected from earthquake-affected areas.
- Hatay binders (H1, H2) showed the lowest penetration, highest softening point, and the greatest viscosity values at both 135 °C and 165 °C, indicating severe hardening, strong rutting resistance, and lower phase angles associated with greater elasticity.
- Kahramanmaraş binders (K1, K2) exhibited the highest penetration, lowest softening point, and lower viscosity values, combined with high phase angles, reflecting a softer, more viscous character and reduced resistance to permanent deformation at elevated temperatures.
- Malatya and Gaziantep binders showed intermediate characteristics; Malatya demonstrated moderate stiffness, while Gaziantep retained greater flexibility.
- Viscosity values decreased significantly with increasing temperature in all samples, and DSR results confirmed a decline in rutting resistance at high temperatures; however, binders with higher initial $G^*/\sin\delta$ values preserved performance more effectively.
- Post-earthquake binder performance was found to be directly influenced by local seismic intensity, climatic conditions, and pavement service history, highlighting the necessity for maintenance and rehabilitation strategies to be tailored to the specific material properties of each region.

5. Author Contribution Statement

In the study carried out, Author 1 contributed to the formation of the idea, making the design and literature review, evaluating the results obtained, obtaining the materials used, and examining the results, spelling and checking the article in terms of content.

6. Ethics Committee Approval and Conflict of Interest

There is no conflict of interest with any person/institution in the prepared article.

7. Ethical Statement Regarding the Use of Artificial Intelligence

No artificial intelligence-based tools or applications were used in the preparation of this study. The entire content of the study was produced by the author in accordance with scientific research methods and academic ethical principles.

8. References

- [1] K. Hacıfendioğlu, and H.B. Başağa, “Concrete road crack detection using deep learning-based Faster R-CNN method,” *Iran. J. Sci. Technol. Trans. Civ. Eng.*, vol. 46, no. 2, pp. 1621–1633, Apr. 2022.
- [2] A.C. Altunışık, M.E. Arslan, V. Kahya, B. Aslan, T. Sezdirmez, G. Dok, O. Kirtel, H. Öztürk, F. Sunca, A. Baltacı, M. Emiroğlu, M. Günaydın, S. Adanur, B. Atmaca, T. Akgül, A. Demir, T. Tatar, B. Aykanat, K. Hacıfendioğlu, A. Sarıbiyik, M. Yurdakul, Y.E. Akbulut, F.Y. Okur, F. Şen, A.F. Genç, H.B. Başağa, E. Demirkaya, O. Güleş, and M. Nas, “Field observations and damage evaluation in reinforced concrete uildings after the February 6th, 2023, KahramanmaraşTürkiye earthquakes,” *J. Earthq. Tsunami*, vol. 17, no. 06, Dec. 2023.
- [3] B. Atmaca et al., “On the earthquake-related damages of civil engineering structures within the areas impacted by Kahramanmaraş earthquakes,” *J. Struct. Eng. Appl. Mech.*, vol. 6, no. 2, Jul. 2023.
- [4] B. Atmaca, M.E. Arslan, M. Emiroğlu, A.C. Altunışık, S. Adanur, A. Demir, M. Günaydın, O. Kirtel, T. Tatar, V. Kahya, F. Sunca, F.Y. Okur, K. Hacıfendioğlu, G. Dok, H. Öztürk, İ. Vural, O. Güleş, A.F. Genç, E. Demirkaya, M. Yurdakul, M. Nas, Y.E. Akbulut, A. Baltacı, B.A. Temel , H.B. Başağa, A. Sarıbiyik, F. Şen, B. Aykanat, İ.Ş. Öztürk, M.B. Navdar, F. Aydın, K. Öntürk, M. Utkucu, and T. Akgü, “Field observations and numerical investigations on seismic damage assessment of RC and masonry minarets during the February 6th, 2023, Kahramanmaraş (Mw 7.7 Pazarcık and Mw 7.6 Elbistan) earthquakes in Türkiye,” *Int. J. Archit. Herit.*, vol. 19, no. 7, pp. 1117–1142, Jul. 2025.
- [5] F. Liu, J. Liu, and L. Wang, “Asphalt pavement crack detection based on convolutional neural network and infrared thermography,” *IEEE Trans. Intell. Transp. Syst.*, vol. 23, no. 11, pp. 22145–22155, Nov. 2022.
- [6] F. Liu, and L. Wang, “UNet-based model for crack detection integrating visual explanations,” *Constr. Build. Mater.*, vol. 322, p. 126265, Mar. 2022.
- [7] Z. Liu, Y. Cao, Y. Wang, and W. Wang, “Computer vision-based concrete crack detection using U-net fully convolutional networks,” *Autom. Constr.*, vol. 104, pp. 129–139, Aug. 2019.
- [8] A. Cubero-Fernandez, F. J. Rodriguez-Lozano, R. Villatoro, J. Olivares, and J. M. Palomares, “Efficient pavement crack detection and classification,” *EURASIP J. Image Video Process.*, vol. 2017, no. 1, p. 39, Dec. 2017.
- [9] G. Doğan, and B. Ergen, “Karayollarındaki asfalt çatlaklarının tespiti için yeni bir konvolüsyonel sinir ağı tabanlı yöntem,” *Firat Univ. Mühendislik Bilim. Derg.*, vol. 34, no. 2, pp. 485–494, Sep. 2022.
- [10] J. Guan, X. Yang, L. Ding, X. Cheng, V. C. S. Lee, and C. Jin, “Automated pixel-level pavement distress detection based on stereo vision and deep learning,” *Autom. Constr.*, vol. 129, p. 103788, Sep. 2021.
- [11] B. Li, K. C. P. Wang, A. Zhang, E. Yang, and G. Wang, “Automatic classification of pavement crack using deep convolutional neural network,” *Int. J. Pavement Eng.*, vol. 21, no. 4, pp. 457–463, Mar. 2020.
- [12] P. Miao ,and T. Srimahachota, “Cost-effective system for detection and quantification of concrete surface cracks by combination of convolutional neural network and image processing techniques,” *Constr. Build. Mater.*, vol. 293, p. 123549, Jul. 2021.
- [13] U. A. Nnolim, “Automated crack segmentation via saturation channel thresholding, area classification and fusion of modified level set segmentation with Canny edge detection,” *Heliyon*, vol. 6, no. 12, p. e05748, Dec. 2020.
- [14] K. Hacıfendioğlu, H. B. Başağa, V. Kahya, K. Özgan, and A. C. Altunışık, “Automatic detection of collapsed buildings after the 6 February 2023 Türkiye earthquakes using post-disaster satellite images with deep learning-based semantic segmentation models,” *Buildings*, vol. 14, no. 3, p. 582, Feb. 2024.
- [15] S. Dorafshan, R. J. Thomas, and M. Maguire, “Comparison of deep convolutional neural networks and edge detectors for image-based crack detection in concrete,” *Constr. Build. Mater.*, vol. 186, pp. 1031–1045, Oct. 2018.

- [16] K. Demir ,and O. Yaman, “A HOG feature extractor and KNN-based method for underwater image classification,” *Firat Univ. J. Exp. Comput. Eng.*, vol. 3, no. 1, pp. 1–10, Feb. 2024.
- [17] F. Demir, E. Yalcin, and M. Yilmaz, “CrackNet: A new deep learning-based strategy for automatic classification of road cracks after earthquakes,” *Eng. Sci. Technol. Int. J.*, vol. 69, p. 102128, Sep. 2025.
- [18] M. Yılmaz; E. Yalçın, S. Kifah, F. Demir, A. Şengür, and R. Demir, All Authors, “Improving the classification performance of asphalt cracks after earthquake with a new feature selection algorithm,” *IEEE Access*, vol. 12, pp. 6604–6614, 2024.
- [19] M. Yilmaz, E. Yalcin, F. Demir, A.M. Ozdemir, M. Atar, A. Gune, “Automatic segmentation of asphalt cracks on highways after large-scale and severe earthquakes using deep learning-based approaches,” *IEEE Access*, vol. 13, pp. 22820–22830, 2025.
- [20] B. F. Yalçın, and M. Yilmaz, “Investigation of the performance of bio-oils from three different agricultural wastes as rejuvenators for recycled asphalt,” *Turkish J. Civ. Eng.*, vol. 35, no. 3, pp. 95–123, May 2024.
- [21] B. F. Yalçın, M. Yilmaz, and H. S. Altundogan, “Experimental investigation of rejuvenated asphalt mixtures using bio-oils from different biomass sources,” *Bitlis Eren Univ. Fen Bilim. Derg.*, vol. 13, no. 4, pp. 988–998, Dec. 2024.
- [22] Ö. Karadağ, and M. Saltan, “Investigation of adhesion and stripping properties of asphalt modified with bio-oil,” *Firat Univ. J. Exp. Comput. Eng.*, vol. 4, no. 2, pp. 262–275, Jun. 2025.
- [23] E. Yalçın, “Investigation of rheological properties of aged polymer modified binders,” *J. Innov. Sci. Eng.*, Apr. 2024.
- [24] H. Aydin, E. Yalçın, M. Yilmaz, and T. Alataş, “Investigation of physical and rheological properties of Elvaloy and polyphosphoric acid modified bitumen,” *Afyon Kocatepe Univ. J. Sci. Eng.*, vol. 22, no. 5, pp. 1122–1128, Oct. 2022.